

Selective Separation of Americium(III), Curium(III), and Lanthanide(III) by Aqueous and Organic Competitive Extraction

Qiang Wu,[#] Huaixin Hao,[#] Yang Liu,[#] Lei-Tao Sha, Wei-Jia Wang, Wei-qun Shi,* Zhipeng Wang,* and Ze-Yi Yan*



Cite This: *Inorg. Chem.* 2024, 63, 462–473



Read Online

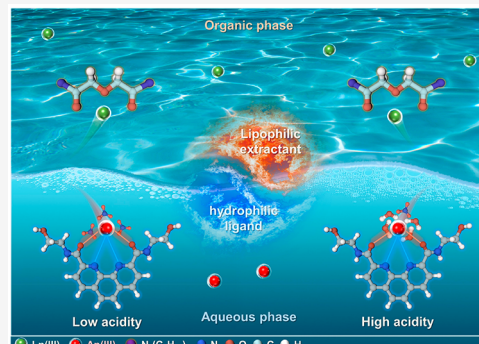
ACCESS |

Metrics & More

Article Recommendations

Supporting Information

ABSTRACT: Adding hydrophilic ligands into aqueous solutions for the selective binding of actinides(III) is acknowledged as an advanced strategy in Ln(III)/An(III) separation. In view of the recycling and radioactive waste disposal of the minor actinide, there remains an urgent need to design and develop the appropriate ligand for selective separation of An(III) from Ln(III). Herein, four novel hydrophilic ligands with hard–soft hybrid donors, derived from the pyridine and phenanthroline skeletons, were designed and synthesized as masking agents for selective complexation of An(III) in the aqueous phase. The known *N,N,N',N'*-tetraoctyl diglycolamide (TODGA) was used as lipophilic extractant in the organic phase for extraction of Ln(III), and a new strategy for the competitive extraction of An(III) and Ln(III) was developed based on TODGA and the above hydrophilic ligands. The optimal hydrophilic ligand of *N,N'*-bis(2-hydroxyethyl)-2,9-dicarboxamide-1,10-phenanthroline (2OH-DAPhen) displayed exceptional selectivity toward Am(III) over Ln(III), with the concentrations of HNO₃ ranging from 0.05 to 3.0 M. The maximum separation factors were up to 1365 for Eu/Am, 417.66 for Eu/Cm, and 42.38 for La/Am. The coordination mode and bonding property of 2OH-DAPhen with Ln(III) were investigated by ¹H NMR titration, UV–vis spectrophotometric titration, luminescence titration, FT-IR, ESI-HRMS analysis, and DFT calculations. The results revealed that the predominant species formed in the aqueous phase was a 1:1 ligand/metal complex. DFT calculations also confirmed that the affinity of 2OH-DAPhen for Am(III) was better than that for Eu(III). The present work using a competitive extraction strategy developed a feasible alternative method for the selective separation of trivalent actinides from lanthanides.



1. INTRODUCTION

The increasing demand of carbon-neutral and low-cost energy has caused nuclear energy to become an essential element in the overall composition of the current global power supply.^{1–4} Accompanied by the high-speed development of nuclear energy, the environmental problems associated with used nuclear fuel have aroused great attention.^{5–7} Of the spent fuel produced by modern light water reactors, over 98.5% of the components are mainly composed of U, Pu, and lanthanides (Ln).⁸ However, it still contains less than 1 wt % of minor actinides (MA) including Am, Np, and Cm, which are responsible for long-standing radiotoxicity.^{9–11} In order to improve the long-term management safety of nuclear waste, the partitioning-transmutation strategy (P&T) was emerged and recognized as a viable global option.^{12,13} The proposed P&T initially partitioned the transuranic elements and long-lived fission products by the PUREX process using solvent extraction,^{14,15} and they were subsequently subjected to neutron bombardment for transmutation into short-lived nuclides.¹⁶ For the realization of the P&T strategy, the initial separation of Ln(III) from An(III) is an inevitable prerequisite.¹⁷ This is due to the fact that some lanthanide isotopes

with large neutron cross sections can hinder the efficient transmutation of minor actinides.^{18,19}

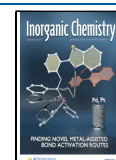
Because of their extremely similar chemical behavior and ionic radius, separation of Ln(III)/An(III) has posed a major challenge in the field of nuclear industry.^{20–23} As evidenced by a series of crystal structures and theoretical analyses of Ln(III)/An(III) complexes, some ligands involving N- or S-donors exhibited the greater affinity for An(III) than Ln(III) through covalent interactions.^{16,24} Therefore, some typical soft ligands with N- or S-donors were widely developed for the selective complexation of An(III) from PUREX raffinate to reprocess minor actinides, such as the TRPO-Cyanex 301 process in China, the SANEX and GANEX processes in Europe, and the TRUEX and TALSPEAK strategies in the USA.^{12,25,26} In these processes, some lipophilic or hydrophilic

Received: September 22, 2023

Revised: December 5, 2023

Accepted: December 5, 2023

Published: December 23, 2023



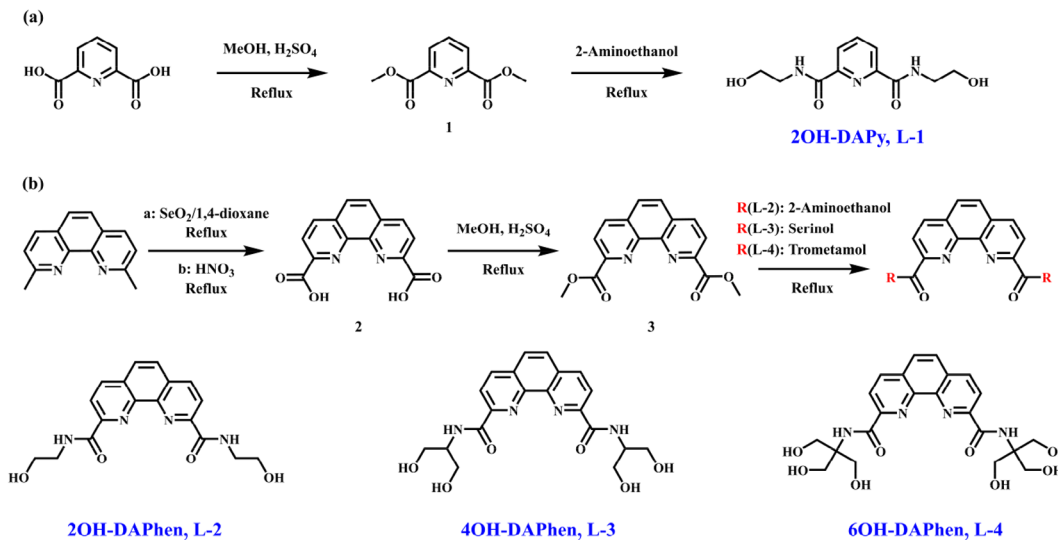


Figure 1. Synthetic route of (a) 2OH-DAPy (L-1) and (b) 2OH-DAPhen (L-2), 4OH-DAPhen (L-3), and 6OH-DAPhen (L-4).

N-donor ligands were elaborately tailored including 2,6-bis(5,6-dialkyl-1,2,4-triazin-3-yl)pyridine, 6,6'-bis(5,6-dialkyl-1,2,4-triazin-3-yl)-2,2'-bipyridine, and 2,9-bis(1,2,4-triazin-3-yl)-1,10-phenanthroline, which exhibited excellent affinity toward MA elements.^{27–29} Nevertheless, there are still certain limitations for these ligands in the separation of An(III), such as their limited solubility in nonpolar *n*-paraffin.^{30,31} Therefore, some volatile and toxic solvents with greater polarity have been put to use for extraction of An(III).³²

The utilization of soft-hard hybrid N,O-ligands has also garnered great attention for the potential in the separation of An(III) and Ln(III).^{33,34} Introduction of the softer N atom endowed the ligands with the better affinity to An(III) than Ln(III) through covalent interaction, while the harder O atom ensured the essential binding ability of ligands to metal ions.^{35,36} As we know, skeletons of pyridine and phenanthroline were used as the most popular platform for introduction of N,O-donors due to inherent preorganized properties and abundant modifiable sites around the central molecules.^{37,38} For instance, the hydrophilic 2,6-pyridinedicarboxylic acid has been employed as an N,O-ligand owing to its good affinity for f-elements.^{35,39} The ligands based on 2,6-pyridine dicarboxamide (DAPy) have frequently found applications as extractants for f-elements and display the potential for the separation of An.^{39,40} The soft-hard donor ligands based on phenanthroline frames also exhibited the outstanding performance in complexing actinide ions of various oxidation states.^{40,41} Among these ligands, *N,N'*-diethyl-*N,N'*-ditoly-9-diamide-1,10-phenanthroline was recognized as a particularly suitable extractant for extracting An(III), which showed the excellent selectivity for MA over Ln(III).⁴²

Recently, an innovative method known as the *i*-SANEX process was developed for the partitioning of An(III)/Ln(III) as a feasible strategy.^{43,44} The *i*-SANEX process used the nonselective TODGA extractant for coextraction of trivalent f-element cations, followed by selectively stripping An(III) into the aqueous phase using a hydrophilic ligand containing N-donors.⁴⁵ Inspired by the above strategy, a more accessible method was developed by adding lipophilic TODGA in the organic phase and hydrophilic complexes into aqueous solution to form a competitive extraction system. This

alternative method not only greatly simplified the process for selective extraction of An(III) but also skillfully avoided the problem of poor solubility in the organic phase frequently encountered in applications of highly selective N-donor ligands. Based on the *i*-SANEX process and the updated strategy, some important hydrophilic masking agents such as pyridine-2,6-bis(1*H*-1,2,3triazol-4-yl),⁴⁵ sulfonated bis-1,2,4-triazine,^{16,46–48} 2,9-bis(1*H*-1,2,3-triazol-4-yl)-1,10-phenanthroline,¹⁷ and *N,N'*-diphenyl-2,9-diamide-1,10-phenanthroline⁴⁹ were designed and synthesized for separation of Am(III) and Eu(III), which exhibited good affinity for Am(III) in the aqueous phase. However, the poor adaptability to high acidity and harsh preparation conditions limited their practicality and industrial availability.^{30,31} Therefore, the evolution of novel ligands for the highly selective complexation of Am(III) from PUREX raffinate was always considered as one of the crucial and formidable challenges encountered in the reprocessing of high-activity waste. Curium(III) is also considered as a key minor actinide in high-level wastes (HLW); separation of Ln(III)/Cm(III) and Am(III)/Cm(III) is also crucial. Although the many above extractants reported permit the coextraction of Am and Cm, their mutual separation can simplify the transmutation of Am.^{50,51}

In this work, the four novel hydrophilic soft-hard hybrid N,O-ligands with 2,6-pyridine dicarboxamide (DAPy) and 2,9-diamide-1,10-phenanthroline (DAPhen) skeletons were designed and synthesized for selective binding of An(III) in the aqueous phase. The known TODGA was used as a lipophilic extractant for the coordination of Ln(III) in organic medium. A biphasic competitive extraction for the separation of An(III)/Ln(III) was developed using the present hydrophilic masking agents and the lipophilic TODGA extractant. The stability constants of complexes of Ln(III) with preferred DAPhen in nitric acid medium were determined through UV-vis spectroscopic titration. To gain insight into the complexation mechanism of the present DAPhen ligands to An(III), DFT calculations, ¹H NMR titration, luminescence titration, ESI-HRMS, and FT-IR analyses were further employed to investigate the coordination mode and bonding properties of DAPhen ligands with various Ln(III).

2. EXPERIMENTAL SECTION

2.1. Chemicals. Chemicals such as methanol (MeOH), 2-aminoethanol, serinol, trometamol, dioxane, selenium dioxide (SeO_2), 2,6-pyridinedicarboxylic acid, 2,9-dimethyl-1,10-phenanthroline, lanthanide nitrates, lanthanide chlorides, and other reagents were obtained commercially and were of analytical grade. The hydrophobic extractant *N,N,N',N'*-tetraoctyl diglycolamide (TODGA) was prepared according to the established method in the previous work.^{49,52} ^{241}Am and ^{244}Cm used as radioactive tracers were provided by the Institute of Nuclear and New Energy Technology (INET), Tsinghua University.

2.2. Synthesis of Hydrophilic Ligands. In this study, the four soft-hard hybrid hydrophilic ligands could be directly synthesized by the amidation reaction of primary amines and carboxylic acid esters. The facile synthesis and simple structure of the present hydrophilic ligands further highlighted their potential in industrial applications.⁵³ The synthetic routes of *N,N'*-bis(2-hydroxyethyl)pyridine-2,6-dicarboxamide (2OH-DAPy, L-1), *N,N'*-bis(2-hydroxyethyl)-2,9-dicarboxamide-1,10-phenanthroline (2OH-DAPhen, L-2), *N,N'*-bis(1,3-dihydroxy-2-propyl)-2,9-dicarboxamide-1,10-phenanthroline (4OH-DAPhen, L-3), and *N,N'*-bis[2-hydroxy-1,1-bis(hydroxymethyl)ethyl]-2,9-dicarboxamide-1,10-phenanthroline (6OH-DAPhen, L-4) are briefly depicted in Figure 1. The synthesis and characterization of the above ligands are displayed in the Supporting Information (SI).

2.3. Extraction Experiments. All radioactive extraction experiments were performed in the specialized facility. In order to simulate the trivalent f-element cations in the PUREX raffinate, traces of ^{241}Am (III) and ^{244}Cm (III) and 0.01 mM of La(III) and Eu(III) were spiked into the desired concentration of HNO_3 solution, which are surrogate for An(III) and Ln(III). The extraction experiments consisted of typical extraction and biphasic competitive extraction, corresponding to the absence and presence of hydrophilic ligands in the aqueous phase, respectively. The organic phase was prepared by dissolving the desired amount of lipophilic extractant in a mixture of kerosene/1-octanol (95/5, v/v). The extraction behavior of the commonly used TODGA (50 mM) for An(III)/Ln(III) was evaluated. In the biphasic competitive extraction experiment, a certain amount of hydrophilic ligand was dissolved in the desired concentration of HNO_3 solution to form a competitive effect with the lipophilic extractant.

An equal volume (usually 0.5 mL) of the aqueous phase and the organic phase were placed in a glass vial and shaken for 30 min at room temperature ($25 \pm 1^\circ\text{C}$) until reaching extraction equilibrium. After the two phases were completely separated by centrifugation (2000 rpm, 2 min), 100 μL of the aqueous phase and the organic phase were taken in 2 mL of scintillation liquid (OptiPhase Hisafe 3), and the activities (in cpm) of α -emitter ^{241}Am were counted using a Quantulus 1220 (PerkinElmer) liquid scintillation counter. The concentration of La(III) and Eu(III) in the aqueous phase before and after extraction was determined by ICP-OES (Agilent 5100, USA). The experiments were performed in triplicate and measured for at least 10 min to ensure the accuracy of the data. The extraction efficiency was interpreted in the distribution ratio (D_M) and defined as the ratio of the concentration of metal ions (radionuclide activity) in the organic phase to the concentration of metal ions (radionuclide activity) in the aqueous phase. The selectivity of Ln(III) against Am(III) was described by the separation factor $SF_{\text{Ln/Am}}$ and defined as the ratio of the $D_{\text{Ln}}/D_{\text{Am}}$.

2.4. NMR Spectroscopy and ^1H NMR Titration. The ^1H NMR (400 MHz, nuclear magnetic resonance) and ^{13}C NMR (100 MHz) spectra of the hydrophilic masking agents, lipophilic extractants, and ^1H NMR titration experiments were collected on a Varian Mercury-400 spectrometer. In the titration experiments, 2OH-DAPhen solutions (L-2, 1.0 mM in CD_3OD) were placed in a series of NMR tubes, and then different volumes of LaCl_3 (25 mM in CD_3OD) or LuCl_3 (25 mM in CD_3OD) solutions were added. The molar ratios of metal ions to hydrophilic masking agent were varied from ~ 0.0 to ~ 3.0 eq. After shaking for 5 min at room temperature ($25 \pm 1^\circ\text{C}$),

the ^1H NMR spectra were then collected for a series of mixtures with different molar ratios.

2.5. UV–Vis Spectrophotometric Titration. The stability constant ($\log \beta$) of the complex of 2OH-DAPhen (L-2) with Nd(III) and the protonation constant (pK_a) of 2OH-DAPhen (L-2) were determined as described in the extraction experiments by UV–vis spectrophotometric titration using a UNICO UV-2355 spectrophotometer at room temperature ($25 \pm 1^\circ\text{C}$). The stock solution of metal ions was prepared in a 0.4 M HNO_3 solution. Typically, 2 mL of 0.05 mM 2OH-DAPhen (L-2) solution was placed in a 10 mm quartz cuvette, and an appropriate aliquot of 1.0 mM $\text{Nd}(\text{NO}_3)_3$ solution was added. The molar ratios of metal ions to hydrophilic masking agent were varied from ~ 0.0 to ~ 3.0 eq. After shaking for 5 min, the titration spectra were collected for a series of samples with different molar ratios. For the determination of the protonation constant, 2 mL of 0.05 mM 2OH-DAPhen (L-2) in deionized water was placed in a 10 mm quartz cuvette, and an appropriate aliquot (usually 10 μL) of 1.0 M HNO_3 solution was added. In order to obtain more accurate pK_a values, the ionic strength of the stock solution was set to 10 mM, and Et_4NNO_3 was used as the background electrolyte. After shaking for 5 min, the titration spectra were collected. The corresponding $\log \beta$ and pK_a values were calculated by a nonlinear regression method fitted with the HypSpec program.

2.6. Luminescence Spectrophotometric and Lifetime Titration. Luminescence emission spectra of Eu(III) titrated with 2OH-DAPhen (L-2) in 1.0 M HNO_3 medium were recorded on an Edinburgh FLS-1000 fluorometer. In general, 2 mL of 1.0 mM $\text{Eu}(\text{NO}_3)_3$ solution was placed in a 10 mm quartz cuvette, and an appropriate aliquot of 20 mM 2OH-DAPhen (L-2) solution was added into the above solution. The molar ratios of masking agent to metal ions were varied from ~ 0.0 to ~ 3.0 eq. After magnetic stirring for 5 min, the titration spectra were collected for the mixture with different molar ratios at the excitation wavelength of 394 nm. Meanwhile, the lifetime decay curves were recorded at the different molar ratios, and the fluorescence lifetimes of the complexes were obtained by fitting with decay analysis software packages. The goodness of fits were evaluated by minimizing the reduced function ($0.7 < \chi^2 < 1.2$). The hydration number of Eu(III) at different molar ratios was calculated according to the correlation between hydration number and lifetime ($N_{\text{H}_2\text{O}} = 1.05/\tau - 0.7$).

2.7. Computational Methods. The methodology employed for the DFT calculation is presented in the Supporting Information.

3. RESULTS AND DISCUSSION

3.1. Competitive Extraction. **3.1.1. Masking Agent Type.** As reported, some hydrophilic ligands have demonstrated favorable selectivity toward Am(III). However, the studies were mainly focused on the selective separation of Am(III) from Eu(III), but little attention was paid to light lanthanides, such as La(III), which are more difficult to separate from Am(III).⁴⁵ Due to the similar extraction ability of popular TODGA to light lanthanides and Am(III), the development of new organic ligands was still required for separating Am(III) from light lanthanides. Based on the soft and hard acid–base theory, we herein developed two types of easily prepared hydrophilic ligands with soft-hard donors, specifically 2OH-DAPy (L-1) and 2OH-DAPhen (L-2), as tri- and tetra-dentate complexants for selective separation of trivalent actinides from trivalent lanthanides. The aim of this study was to compare the complexation potential of DAPhen and DAPy skeletons to metal ions as well as to exploit the inherent hydrophilicity of hydroxyl groups. As expected, both 2OH-DAPy (L-1) and 2OH-DAPhen (L-2) showed good solubility in dilute nitric acid solutions (more than 30 mM), indicating their potential for complexation of Am(III) in the aqueous solution.

In comparison to TBP for industrial applications, DGAs-type ligands, especially TODGA, exhibited the better

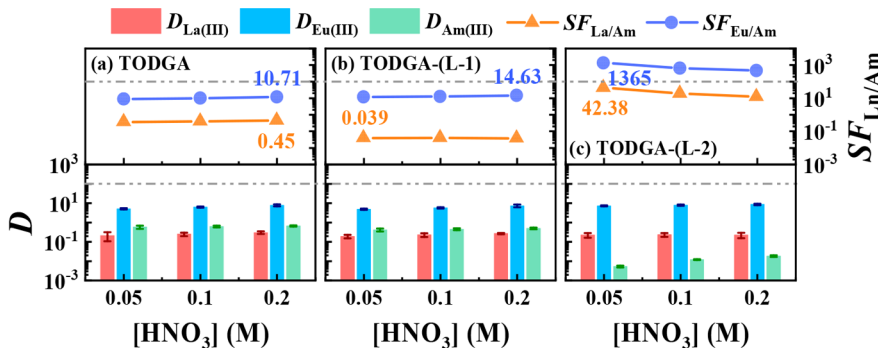


Figure 2. Distribution ratios of Am(III), La(III), and Eu(III) by TODGA in the absence (a) and presence of hydrophilic ligands (b and c). Organic phase, [TODGA] = 50 mM; aqueous phase, [Eu(III)] = [La(III)] = 1×10^{-5} M, L-1 = L-2 = 0.5 mM.

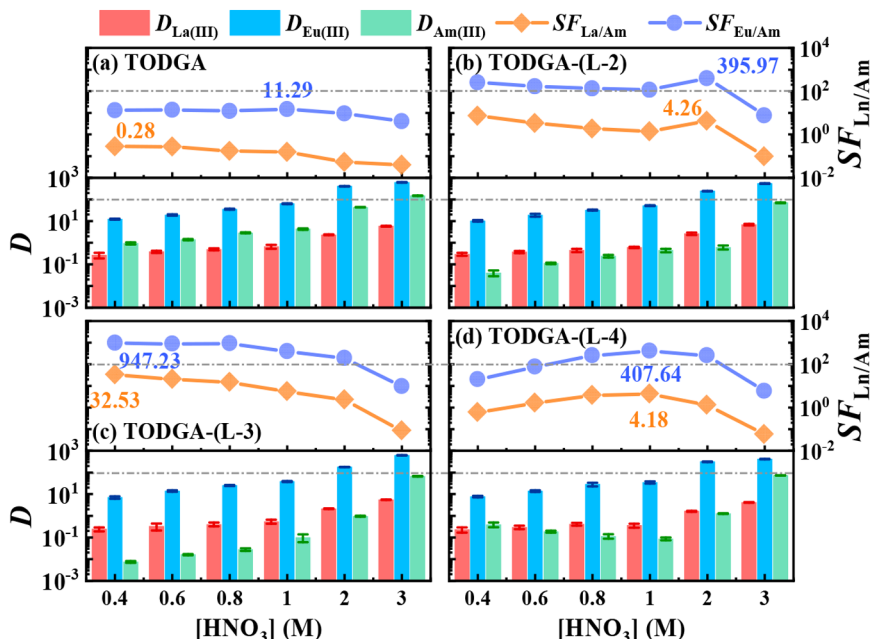


Figure 3. Distribution ratios of Am(III), La(III), and Eu(III) by TODGA in the absence (a) and presence of hydrophilic ligands (b–d). Organic phase, [TODGA] = 50 mM; aqueous phase, [Eu(III)] = [La(III)] = 1×10^{-5} M. [NaNO₃] = 1.0 M, L-2 = L-3 = L-4 = 0.5 mM.

extraction ability for f-elements, therefore, TODGA was selected as an appropriate model to develop the novel two-phase competitive extraction. To improve the extraction performance of 50 mM TODGA to trivalent metal ions under low-acidity conditions, a salting-out agent (1.0 M NaNO₃) was added to the aqueous phase in the present extraction experiments. As revealed in Figure 2a, TODGA without the masking agent exhibited the good affinity for Eu(III) and poor extraction ability to La(III) and Am(III) at low nitric acid concentrations. Introduction of 2OH-DAPy (L-1) into the aqueous phase only lightly increased the maximum SF_{Eu/Am} values to 14.63 from 10.71, indicating that 2OH-DAPy (L-1) is not a suitable masking agent for Am(III) (Figure 2b). Fortunately, the maximum SF_{Eu/Am} values jumped to 1365 from 10.61, and the maximum SF_{La/Am} values also increased from 0.45 to 42.38 in the presence of 2OH-DAPy (L-2). In comparison with 2OH-DAPy (L-1), the 2OH-DAPhen (L-2) masking agent was found to be highly selective for Am(III) against Eu(III) and La(III). As seen in Figure 2c, the biphasic competitive extraction could not significantly increase the D_{Eu} value, and the excellent SF_{Eu/Am} values were due to the sharp

decrease of the D_{Am} value. It was evident that 2OH-DAPhen (L-2) could selectively bind to Am(III) rather than Ln(III), resulting in the higher separation factors of Am(III) to Ln(III). In view of the excellent selectivity for Am(III) over Eu(III) and La(III), the DAPhen-type ligands emerged as a prominent candidate for subsequent study.

3.1.2. DAPhen-Based Masking Agents. After the hydrophilic 2OH-DAPhen (L-2) was recognized as the suitable masking agent for separation of Am(III) and Ln(III), two additional ligands, 4OH-DAPhen (L-3) and 6OH-DAPhen (L-4) were further synthesized and were used as water-soluble masking agents to evaluate their selectivity toward Am(III) and Ln(III). The ligands from L-2 to L-4 were expected to further enhance their solubility in aqueous solution owing to an increasing number of hydroxyl groups. Surprisingly, more hydroxyl groups did not lead to the better water solubility. Among the above three DAPhen ligands, the most soluble ligand in aqueous solution is still 2OH-DAPhen (L-2), which can easily dissolve in neutral to acidic aqueous solutions. It was assumed that the solubility of ligands depended not only on

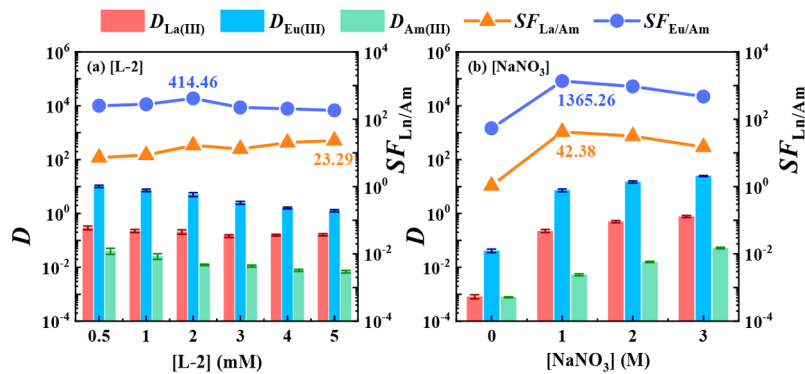


Figure 4. Distribution ratios of Am(III), La(III), and Eu(III) by TODGA with the different concentrations of (a) L-2 and (b) NaNO₃. [Eu(III)] = [La(III)] = 1×10^{-5} M; organic phase, [TODGA] = 50 mM; (a) aqueous phase, [HNO₃] = 0.4 M, [L-2] = 0.5–5.0 mM, [NaNO₃] = 1.0 M; (b) [HNO₃] = 0.05 M, [L-2] = 0.5 mM, [NaNO₃] = 0.0–3.0 M.

the number of hydroxyl groups but also on the steric structure of the ligand.

As depicted in Figure 3, all three DAPhen masking agents exhibited good affinity for Am(III) in aqueous solution. In the presence of hydrophilic ligands, the extraction efficiency of TODGA to Am(III) was significantly suppressed. Compared to the routine TODGA system, the separation factors for Eu(III)/Am(III) in a TODGA–DAPhen competing system were greatly increased under different acidity levels, such as maximum $SF_{\text{Eu/Am}}$ values from 11.29 to 395.97 for 2OH-DAPhen (2.0 M HNO₃), from 11.29 to 947.23 for 4OH-DAPhen (0.4 M HNO₃), and from 11.29 to 407.64 for 6OH-DAPhen (1.0 M HNO₃). As seen, the D_{Am} values gradually increased with increase of the HNO₃ concentration. It indicated that the coordination ability of both 2OH-DAPhen (L-2) and 4OH-DAPhen (L-3) with Am(III) showed an apparently declining tendency, which was ascribed to the partial protonation of the N-donors (Figures 3b and 3c). For the 6OH-DAPhen ligand, the D_{Am} values exhibited a trend of first rising and then falling, and the minimum $D_{\text{Am(III)}}$ values were obtained in a 1.0 M HNO₃ solution. As observed in Figures 3a–3d, the distribution ratios of Am(III) in the presence of hydrophilic ligands at 3.0 M HNO₃ roughly reached the values without DAPhen complexes. It suggested that DAPhen ligands would not act as masking agents to complex with Am(III) due to the complete protonation of the N-donors under higher than 3.0 M nitric acid. In terms of the $SF_{\text{Eu/Am}}$ values, three competitive extraction systems were obviously different. As shown in Figure 3c, the $SF_{\text{Eu/Am}}$ values continually decreased with the increase of HNO₃ concentration in the TODGA-(L-3) system. The TODGA-(L-4) system showed a trend of first increasing and then decreasing, contrary to the D_{Am} values. In the case of the TODGA-(L-2) system, a sudden jumping of the $SF_{\text{Eu/Am}}$ values was observed at the 2.0 M HNO₃ solution. In view of better solubility in aqueous solution, 2OH-DAPhen (L-2) was selected as the candidate for further investigations.

3.1.3. Effect of 2OH-DAPhen Concentration. The masking effect of 2OH-DAPhen (L-2) to Am(III) in 0.4 M HNO₃ using TODGA extractant (50 mM) was further investigated in the presence of 0.5–5.0 mM 2OH-DAPhen (L-2). As shown in Figure 4a, the D_{Eu} and D_{Am} values significantly decreased with the increase of the concentration of 2OH-DAPhen (L-2), and the $D_{\text{La(III)}}$ values displayed a relatively smaller change from 0.5 to 5.0 mM 2OH-DAPhen (L-2). In general, the

distribution ratios of all three metal ions exhibited a decreasing trend with increasing the concentration of masking agent, indicating that introduction of excess 2OH-DAPhen would lead to the lower extraction ability of TODGA to metal ions. The optimal $SF_{\text{Eu/Am}}$ value in 414.46 was obtained using 2.0 mM of 2OH-DAPhen (L-2) and decreased to 182.85 with 5 mM L-2. As distinguished from the $SF_{\text{Eu/Am}}$ values, the $SF_{\text{La/Am}}$ values showed a gradual upward trend up to 23.29 when 0.5–5.0 mM of 2OH-DAPhen (L-2) was loaded into the aqueous solution. The above results clearly displayed the great potential of 2OH-DAPhen (L-2) in the field of Ln(III)/An(III) separation.

3.1.4. Effect of Salting-Out Agent Concentration. The $SF_{\text{Eu/Am}}$ and $SF_{\text{La/Am}}$ values could be improved by the loading of the salting-out agent (NaNO₃) in aqueous solution. As seen in Figure 4b, the introduction of NaNO₃ (1.0–3.0 M) in the competitive extraction system of TODGA-(L-2) significantly enhanced the extraction efficiency of metal ions and greatly increased the separation factors of Ln(III) to Am(III). The maximum $SF_{\text{Eu/Am}}$ and $SF_{\text{La/Am}}$ values were obtained using 1.0 M NaNO₃ as the salting-out agent. However, when the concentration of NaNO₃ was greater than 1.0 M, a gradual decreasing trend in the separation factors was observed, which was attributed to the faster increase of the $D_{\text{Am(III)}}$ values compared to the $D_{\text{Eu(III)}}$ and $D_{\text{La(III)}}$ values. It was clear that the presence of 1.0 M NaNO₃ not only enhanced the distribution ratio and separation factors of metal ions but also effectively facilitated the binding of Am(III) with 2OH-DAPhen (L-2) in the aqueous phase. Therefore, as mentioned above (Section 3.1.1), the 1.0 M NaNO₃ as the salting-out agent was added into the aqueous phase for performing the routine extraction experiments.

3.1.5. Extraction Performance of ²⁴⁴Cm(III). The reprocessing and fabrication of fresh nuclear fuel pose significant challenges due to the short-lived nature of all curium isotopes in spent nuclear fuel, resulting in high neutron dose rates, activity levels, and thermal loads. In addition to the Ln(III)/Am(III) separation, it is crucial to separate Ln(III) and Cm(III) as well as Am(III) and Cm(III) as they belong to trivalent An(III) with similar ionic radii, making their separation extremely difficult. It was expected that the exceptional selectivity of 2OH-DAPhen to Am(III) can be further demonstrated by performing Am(III)/Cm(III) extraction separation. As shown in Table 1, the separation of Eu(III) and Cm(III) was effectively achieved in the TODGA-(L-2)

Table 1. Distribution Ratios of Cm(III) and Separation Factor of $SF_{Eu/Cm}$ and $SF_{Cm/Am}$

organic phase	[TODGA] = 50 mM	
aqueous phase	blank	[L-2] = 0.5 mM ^a
D_{Cm-244}	0.71 ± 0.05	0.02 ± 0.01
$SF_{Eu/Cm}$	7.24 ± 0.10	417.66 ± 0.51
$SF_{Cm/Am}$	1.21 ± 0.20	3.27 ± 0.51

^a[Eu(III)] = 1 × 10⁻⁵ M, [HNO₃] = 0.05 M, (a) added salting-out agent in the aqueous phase, [NaNO₃] = 1.0 M.

competing system. Moreover, the hydrophilic 2OH-DAPhen (**L-2**) exhibited a slight difference in the complexing of Cm(III) and Am(III). Compared to the results without 2OH-DAPhen (**L-2**), the $SF_{Eu/Am}$ values jumped to the maximum 417.66 from 7.24, and the $SF_{Cm/Am}$ values increased to the maximum 3.27 from 1.21. Therefore, the present competitive extraction exhibited efficiency not only in the partitioning of Eu(III)/Am(III) but also demonstrated the potential in Eu(III)/Cm(III) separation.

3.2. Complexation Behavior. **3.2.1. UV–Vis Spectrophotometric Titration.** In order to understand the complexing behavior between 2OH-DAPhen (**L-2**) and trivalent metal ions, a UV–vis spectrophotometric titration method was used to evaluate the spectrographic property in a 0.4 M HNO₃ solution. In view of their similarity in ionic radii, Nd(III) was chosen as an analogue of Am(III) for this study. The UV–vis spectra of the ligands at different Nd(III) equivalents are presented in Figure 5a, while the corresponding stabilization constants for the complexes of 2OH-DAPhen (**L-2**) and Nd(III) are summarized in Table 2. With the rising of concentration of Nd(III), the absorption peak intensity of 2OH-DAPhen (**L-2**) at 256.5 nm exhibited a continuous increase, while the absorption peak at 276.5 nm underwent a red shift to 279.5 nm and tended to diminish, resulting in the formation of an iso-absorption point at 264.5 nm. The above results suggested that a new species was formed during the titration process. The optimal coordination ratio and stability constant of 1:1 (metal:ligand) were obtained by HypSpec analysis. The fitting molar absorptivities and species fractions are presented in Figures 5b and 5c, respectively. These results supported the formation of a 1:1 complex species. With the continuous addition of metal ions, the free ligand demonstrated a tendency to be gradually consumed. At 3.0 equiv metal ions, approximately 10% of the free ligand remained,

indicating a limited extraction capacity for Ln(III) by 2OH-DAPhen (**L-2**).

3.2.2. 1H NMR Titration Studies. The 1H NMR titration experiment was recognized as an effective approach for the comprehensive assessment of complexes of organic ligand and metal ions. In order to understand the composition and structural characteristics of the corresponding complexes, 1H NMR titration experiments of 2OH-DAPhen (**L-2**) in D₂O/0.4 M HNO₃ solutions were further carried out using antimagnetic Lu(NO₃)₃ instead of paramagnetic Nd(III), aiming to elucidate the complexation behavior of trivalent lanthanides and actinides with hydrophilic ligands in aqueous solution. The 1H NMR spectrum of 2OH-DAPhen (**L-2**) in the absence and presence of Lu³⁺ was investigated, and the chemical shift from 2.80 to 9.75 ppm is depicted in Figures 6a and 6b. The starting three peaks with chemical shifts of 8.50–8.52, 8.15–8.17, and 7.78 ppm were attributed to the respective protons H(a), H(b), and H(c) of 2OH-DAPhen (**L-2**). By the introduction of Lu(NO₃)₃, three new peaks (denoted by blue circles) were observed, and the intensity of the peaks gradually increased with increasing the Lu(NO₃)₃ amount. Meanwhile, the intensity of the starting three peaks (denoted by black triangles) exhibited a decreasing trend and gave the greater chemical shifting. The appearance of three new peaks clearly suggested the formation of new species between 2OH-DAPhen (**L-2**) and Lu³⁺. Except the peaks labeled by blue circles, no other peak was observed when loading 0.2 equiv to 2.0 equiv Lu(III). Combined with UV–vis spectrophotometric titration, it was apparent that 2OH-DAPhen (**L-2**) and Ln(NO₃)₃ form a 1:1 complex by the complex reaction.

3.2.3. Study on 2OH-DAPhen-Nd(III) Complex. In order to further investigate the complexation behavior of 2OH-DAPhen with trivalent metal ions, FT-IR spectroscopic and ESI-HRMS analyses were used to investigate the aqueous phase after competitive extraction of metal ions in a 0.4 M HNO₃ medium. As shown in Figure 7a, the $\nu(C=O)$ peak at 1655 cm⁻¹ of 2OH-DAPhen (**L-2**) underwent a red shift to 1634 cm⁻¹ after coordination of Nd(III) ions, indicating that the carbonyl group of the 2OH-DAPhen (**L-2**) ligand was involved in the complex reaction. The $\nu(C=N)$ peak at 1541 cm⁻¹ of 2OH-DAPhen (**L-2**) blue-shifted to 1570 cm⁻¹, and the shifting of 29 cm⁻¹ in the C=N frequency suggested a strong interaction of N atoms with Ln(III) ions. The ESI-HRMS analysis of the 2OH-DAPhen-Nd(III) complex in positive ion

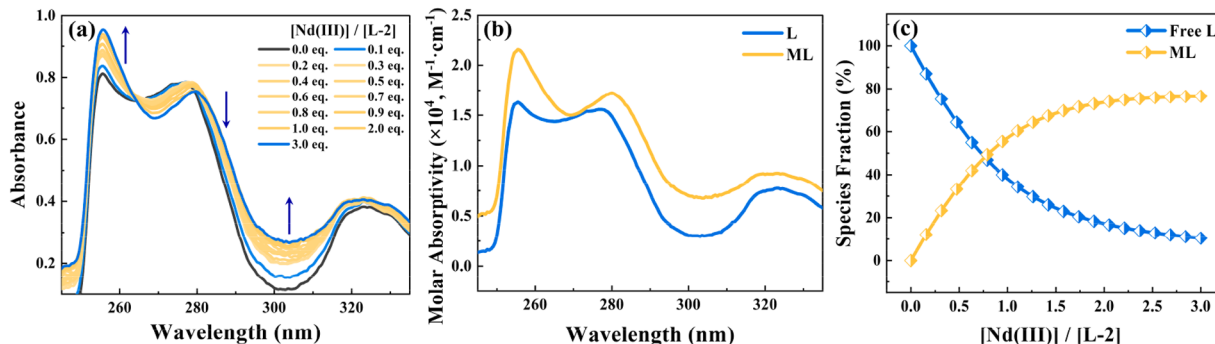


Figure 5. UV–vis spectrophotometric titration spectra of **L-2** with (a) Nd(III) and (b) HNO₃. Titration parameters: (a) initial solution, $V^0 = 2.0$ mL; $C_L^0 = 0.05$ mM in 0.4 M HNO₃; titrant, $C_{Nd(III)}^0 = 1.0$ mM in 0.4 M HNO₃. (b) Fitted molar absorptivity and (c) species fraction of the 2OH-DAPhen-Nd(III) complex.

Table 2. Stability Constants ($\log \beta$) and Protonation Constants (pKa) for the Complexation Reactions of Nd(III) and H⁺ with L-2 in HNO₃ Solution

titrant	ligand	reaction	$\log \beta/\text{pKa}$	ionic medium
Nd(III)	L-2	$\text{L-2} + \text{Nd}^{3+} \rightleftharpoons \text{Nd(L-2)}^{3+}$	4.31 ± 0.04	0.4 M HNO ₃
HNO ₃	L-2	$\text{H(L-2)}^+ \rightleftharpoons \text{L-2} + \text{H}^+$	1.64 ± 0.01	10 mM Et ₄ NNO ₃
HNO ₃	L-1	$\text{H(L-1)}^+ \rightleftharpoons \text{L-1} + \text{H}^+$	1.74 ± 0.02	10 mM Et ₄ NNO ₃

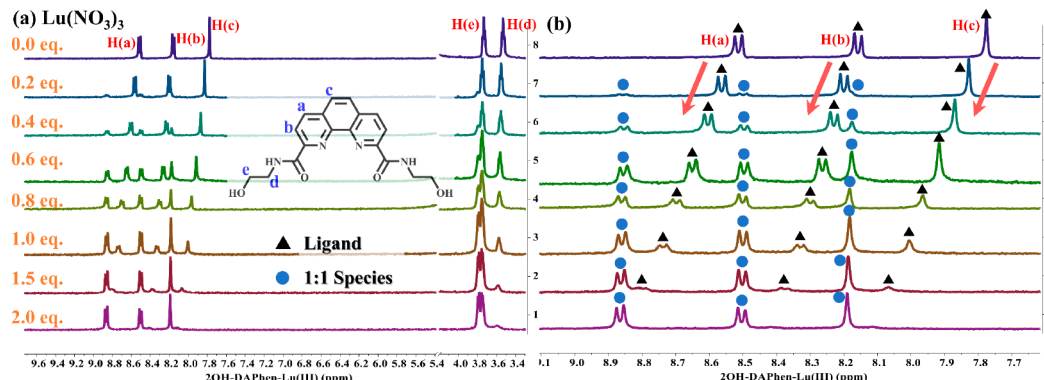


Figure 6. Stacked ¹H NMR spectra of L-2 (5.0 mM) titrated with (a and b) Lu(III) in D₂O/0.4 M HNO₃. Titration parameters: initial solution, $V^0 = 0.6 \text{ mL}$; $C_{\text{L}}^0 = 5.0 \text{ mM}$; titrant, $C_{\text{La(III)}}^0 = C_{\text{Lu(III)}}^0 = 100 \text{ mM}$.

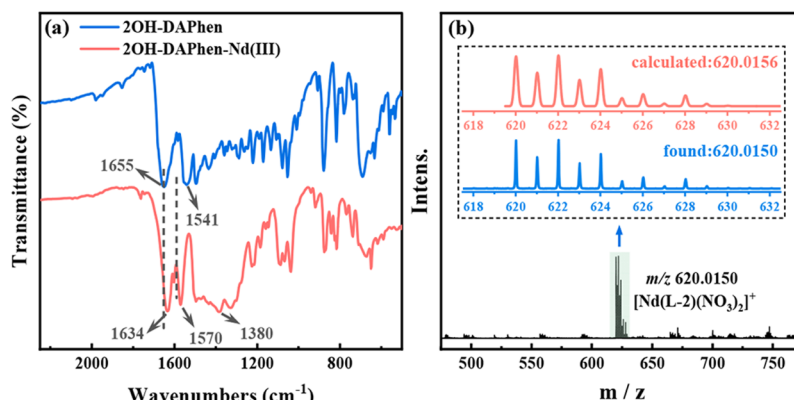


Figure 7. (a) FT-IR spectra of 2OH-DAPhen (L-2) and the 2OH-DAPhen-Nd(III) complex in 0.4 M HNO₃; (b) ESI-HRMS spectra of the 2OH-DAPhen-Nd(III) complex in 0.4 M HNO₃.

mode is displayed in Figure 7b. Within the range of 450 to 800 m/z , a prominent group of cation peaks was observed. The primary peak appeared at 620.0150 m/z , accompanied by the corresponding isotopic peaks at 621.0125, 622.0239, 623.0204, 624.0176, 625.0314, 626.0303, 627.0458, and 628.0303 m/z , which was in good agreement with the theoretical value of $[\text{Nd(L-2)}(\text{NO}_3)_2]^+$ ($\text{C}_{18}\text{H}_{18}\text{N}_6\text{NdO}_{10}^+$, calcd. 620.0156). Combined with the results from UV-vis titrations and ¹H NMR titrations, it was evident that the complex of 2OH-DAPhen (L-2) and Ln(III)/Am(III) under low-acid conditions corresponded to the $\text{M}(2\text{OH-DAPhen})(\text{NO}_3)_3$ species.

3.2.4. Luminescence Titration. As we know, the nitrogen donor ligands possess a certain degree of basicity and tend to protonate in acidic solutions, which would result in the lower selectivity to metal ions. However, the present competitive extraction system of TODGA-(L-2) always exhibited good selectivity toward Am(III) even under a highly acidic medium. To further elucidate the coordination mode of 2OH-DAPhen (L-2) with trivalent metal ions, Eu(III)-based luminescence

titration was conducted in a 1.0 M HNO₃ solution, similar to the condition of extraction.

The unique luminescence property of Eu(III) provided a good method to study the complexation behavior of 2OH-DAPhen (L-2) with trivalent metal ions. The $^5\text{D}_0 \rightarrow ^7\text{F}_J$ ($J = 0-6$) transition of Eu(III) revealed the prominent photoluminescence in the red region, and the intensity of the emission band was closely related to the high-frequency vibration in the first coordination layer of Eu(III). The luminescence emission spectra of Eu(III) in different molar ratios are displayed in Figure 8a. The observed emission bands at approximately 592, 616, and 697 nm were assigned to the transitions of $^5\text{D}_0 \rightarrow ^7\text{F}_1$, $^5\text{D}_0 \rightarrow ^7\text{F}_2$, and $^5\text{D}_0 \rightarrow ^7\text{F}_4$, respectively. The emission intensity of all three bands increased with the increase of ligand concentration, and the transition from $^5\text{D}_0 \rightarrow ^7\text{F}_2$ showed the greater sensitivity to the coordination environment. In addition, the emission intensity also exhibited a rapid increase as the molar ratios of ligand to metal ions increased from 0 to 1.0. However, the increase rate of emission intensity gradually slows down when the molar

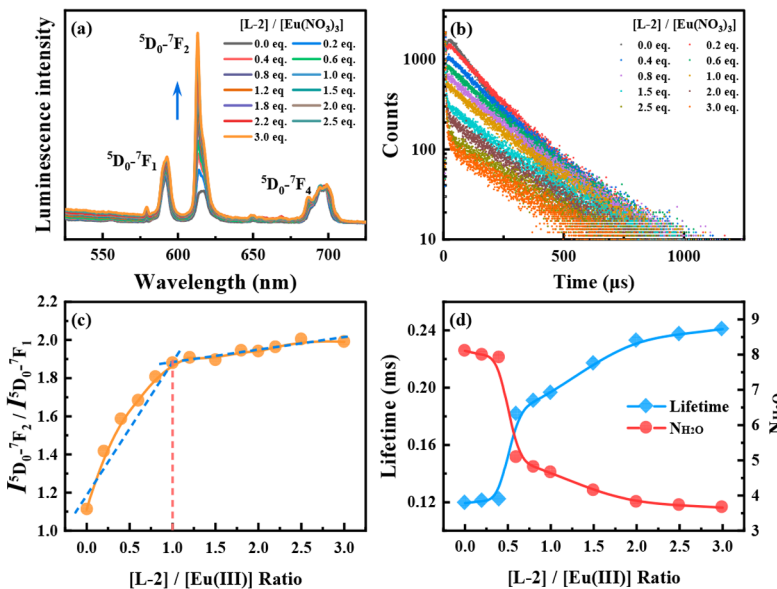


Figure 8. Luminescence titration for the complexation of $\text{Eu}(\text{NO}_3)_3$ with L-2 in 1.0 M HNO_3 . Titration parameters: initial solution, $V^0 = 2.0 \text{ mL}$; $C_{\text{Eu}(\text{III})}^0 = 1.0 \text{ mM}$; titrant, $C_L^0 = 20 \text{ mM}$. (a) Change of the luminescence emission spectra with different molar ratios; (b) change of the luminescence lifetime decay curves with different molar ratios; (c) the ratios of emission intensity of the ${}^5\text{D}_0 \rightarrow {}^7\text{F}_2$ transition ($I({}^5\text{D}_0 \rightarrow {}^7\text{F}_2)$) to emission intensity of the ${}^5\text{D}_0 \rightarrow {}^7\text{F}_1$ transition ($I({}^5\text{D}_0 \rightarrow {}^7\text{F}_1)$) as a function of the molar ratios; and (d) the corresponding luminescence lifetime and hydrated water number as a function of the molar ratios.

ratio was higher than 1.0. As seen in Figure 8c, the asymmetry factor ($AF = I({}^5\text{D}_0 - {}^7\text{F}_2)/I({}^5\text{D}_0 - {}^7\text{F}_1)$) has a distinct inflection point at the molar ratio of 1.0, indicating that the asymmetry of the coordination environment of Eu(III) and 2OH-DAPhen tended to be stable at the complexation ratio of 1:1. The formation of a 1:1 complex was consistent with the previous results obtained from UV-vis spectrophotometric titration, ¹H NMR titration, and ESI-HRMS.

In the first coordination sphere of Eu(III), the vibration of the hydroxyl group combined to Eu(III) could produce a quenching effect, thereby shortening the luminescence lifetime of Eu(III). The structure of the Eu(III)-2OH-DAPhen complex might be roughly inferred by measuring the luminescence decay curve and the corresponding average fluorescence lifetime during titration of 2OH-DAPhen (L-2) with Eu(III). The luminescence decay curves during titration are presented in Figure 8b, and the average lifetime was determined through fitting the curve. As shown in Figure 8d, the average fluorescence lifetime of Eu(III) increased with the increase of the molar ratio, suggesting that the water molecules were gradually replaced by the ligand molecules during the titration process. The average hydration number was calculated by the relationship between hydration number and the lifetime. During the titration process, the number of water molecules around the Eu(III) center decreased from the initial 9 ± 0.5 to the final 4 ± 0.5 , assuming that $[\text{M}(\text{L-2})(\text{H}_2\text{O})_4\text{NO}_3]^{2+}$ may be the possible binding species under strongly acidic conditions.

3.3. DFT Modeling. The structures of the L-1 and L-2 ligands were optimized at the B3LYP/6-31G(d,p) level of theory. The electrostatic potential (ESP) plots of the L-1 and L-2 ligands are shown in Figure 9. The red area and blue area indicated the negative and the positive ESP, respectively. As seen from the ESP plot, the red area was mainly located in the central cavity of the ligands, which was composed of pyridine or phenanthroline N atoms and amide O atoms. The

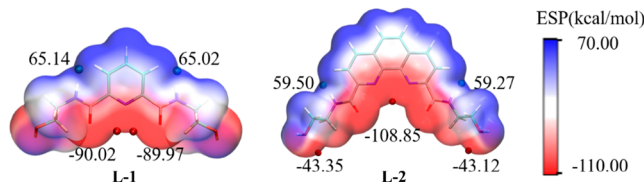


Figure 9. ESP plots of the optimized L-1 and L-2 ligands at the B3LYP/6-31G(d,p) level of theory in the aqueous phase.

concentration of electrons in the red area indicated that the N and O atoms of the ligand were the main donor atoms of the ligand. The L-2 ligand (-108.85 kcal/mol) has more negative electrostatic potential values than the L-1 ligand (-90.92 kcal/mol), suggesting that the L-2 ligand has a stronger affinity for metal ions.

According to the fluorescence spectroscopic study, the possible 1:1 binding species $[\text{ML}(\text{H}_2\text{O})_4\text{NO}_3]^{2+}$ were explored at the B3LYP/6-31G(d,p)/RECP level of theory in the aqueous phase. Meanwhile, the possible 1:1 and 1:2 type binding species $\text{ML}(\text{NO}_3)_3$ and $[\text{ML}_2(\text{NO}_3)]^{2+}$ under high acidity were also investigated at the same level of theory. The optimized geometrical structures of the $[\text{ML}(\text{H}_2\text{O})_4\text{NO}_3]^{2+}$, $\text{ML}(\text{NO}_3)_3$, and $[\text{ML}_2(\text{NO}_3)]^{2+}$ complexes are shown in Figure 10. The results demonstrated that both two ligands coordinated to the Am(III)/Eu(III) via the nitrogen atoms of the phenanthroline/pyridine ring and the oxygen atoms of the amide. The L-1 ligand is a tridentate ligand, while the L-2 ligand is a tetradeятate ligand. The M-L complexes of ligands and metal ions formed 9/10-coordinated complexes with the participation of water molecules and the bidentate nitrate ions.

The average bond distances of the M–N, M–O_(L), M–O_(H₂O), and M–O_{(NO₃)[−]} bonds for $[\text{ML}(\text{H}_2\text{O})_4\text{NO}_3]^{2+}$, $\text{ML}(\text{NO}_3)_3$, and $[\text{ML}_2(\text{NO}_3)]^{2+}$ complexes are displayed in Table S2. The bond distances of the M–O_(L) bonds were shorter than the M–N bonds, suggesting that the coordination

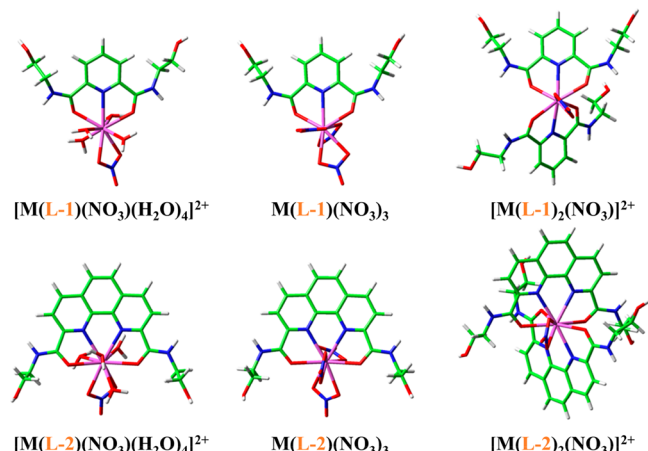


Figure 10. Optimized geometrical structures of the $[\text{ML}(\text{H}_2\text{O})_4\text{NO}_3]^{2+}$, $\text{ML}(\text{NO}_3)_3$, and $[\text{ML}_2(\text{NO}_3)]^{2+}$ complexes in the aqueous phase. The H, C, N, O, and M atoms are represented by white, green, blue, red, and pink, respectively.

ability of amide oxygen atoms was stronger than the nitrogen atoms of the phenanthroline/pyridine ring. In addition, all the bond distances of the M–N, M–O_(L), M–O_(H₂O), and M–O_(NO³⁻) bonds in the Am–ligand complexes were longer than those of the Eu–ligand complexes. In view of the larger ionic radius of Am(III) (1.070 Å) than that of Eu(III) (0.995 Å), it is clear that the Am–N and Am–O bonds have the stronger interaction than those of the Eu–ligand complexes. Since the L-1 ligand has less N donor atoms than the L-2 ligand, that is to say, the formation of a smaller coordination cavity, the M–N and M–O bond distances of the M–(L-1) complexes are shorter than those of the M–(L-2) complexes.

The bonding natures of the M–N, M–O_(L), M–O_(H₂O), and M–O_(NO³⁻) bonds for the $[\text{ML}(\text{H}_2\text{O})_4\text{NO}_3]^{2+}$, $\text{ML}(\text{NO}_3)_3$, and $[\text{ML}_2(\text{NO}_3)]^{2+}$ complexes were declared by the Mayer bond order (MBO) and quantum theory of atoms in molecule (QTAIM), which are listed in Tables S3 and S4, respectively. The MBO of the M–O_(L) bonds was larger than that of the M–N bonds, indicating that the coordination ability of amide oxygen atoms was stronger than the nitrogen atoms of phenanthroline/pyridine, which was consistent with bond distance analysis. The MBO of the M–N bond in the Am–L and Eu–L complexes was close, while the MBO of the Am–O bond was higher than that of the Eu–O bond. QTAIM can provide insightful information at the bond critical point (BCP), and the related parameters including electronic density (ρ), Laplacian of electron density ($\nabla^2\rho$), and energy density (H) are presented in Table S3. Since $\rho < 0.10$ au and $\nabla^2\rho > 0$ indicated an ionic bond, the M–N and M–O bonds were the main ionic interaction. The values of ρ at the M–O_(L) BCPs were larger than those at the M–N BCPs, which revealed that amide O atoms have stronger complexation ability with trivalent metal ions compared to the nitrogen atoms of phenanthroline/pyridine. It could be seen that the value of ρ in the Am–L complex was greater than that of the Eu–L complex, which suggests that the affinity of the ligand to Am(III) was stronger than that of Eu(III). For the values of energy density at the BCPs, most of the Am–L complexes were negative, while most of the Eu–L complexes were positive, revealing that Am–L complexes have more covalent interactions in bonding than Eu–L complexes. The results

were in agreement with the previous bond distance and MBO analysis.

To gain a better understanding of the extraction process, the Gibbs free energy of the possible extraction reaction was further calculated (Table S5). TODGA mainly forms 1:3 (Am:L) type complexes in the organic phase. Since the optimization of the Am(III) complexes with TODGA ligands was very time-consuming, we used tetramethyldiglycolamide (TMDGA) instead of TODGA for the present theoretical calculation. As shown in Table S5, the values of ΔG for all the extraction reactions were negative within the range of -54 to -104 kcal/mol, which suggested that the L-1 and L-2 ligands have significant extraction capabilities for Am(III) and Eu(III) ions. The Am–L complexes have more negative ΔG values than the Eu–L complexes, which suggested that these ligands more easily stripped Am(III) from the $[\text{Am}(\text{TMDGA})_3]^{3+}$ complex than Eu–L complexes. Further, all the free energy of the Am–(L-2) complexes were more negative than the corresponding Eu–(L-2) complexes, revealing that the extraction capacity of the ligand L-2 was stronger than that of the L-1 ligand. According to the $\Delta\Delta G$ ($\Delta\Delta G = \Delta G_{\text{Am}} - \Delta G_{\text{Eu}}$) value of the reaction, the separation effect of the L-2 ligand was stronger than that of L-1, and the reaction $\Delta\Delta G$ of the $[\text{ML}(\text{H}_2\text{O})_4\text{NO}_3]^{2+}$ complex was more negative than that of the $\text{ML}(\text{NO}_3)_3$ and $[\text{ML}_2(\text{NO}_3)]^{2+}$ complexes, indicating that the formation of the $[\text{ML}(\text{H}_2\text{O})_4\text{NO}_3]^{2+}$ complex could enhance the efficiency of An(III)/Ln(III) separation.

4. CONCLUSIONS

The four new hydrophilic soft and hard hybrid ligands derived from DAPhen and DAPy, namely 2OH-DAPy, 2OH-DAPhen, 4OH-DAPhen, and 6OH-DAPhen as masking agents, were investigated for the separation of An(III) from Ln(III) in the TODGA extraction system. Among these hydrophilic ligands, 2OH-DAPhen exhibited a better affinity to An(III) over Ln(III) across a range of nitric acid concentrations (0.05–3.0 M) with very high selectivity. In the optimal condition, the values of $SF_{\text{Eu/Am}}$, $SF_{\text{La/Am}}$, and $SF_{\text{Eu/Cm}}$ were determined to be 1365, 42.38, and 417.66, respectively. Remarkably, even at a higher HNO₃ concentration of 2.0 M, the $SF_{\text{Eu/Am}}$ still reached a significant value of 395.97. The extraction mechanism for the formation of a 1:1 complex between 2OH-DAPhen and Ln(III) was investigated through comprehensive analytic techniques including ¹H NMR titration, ESI-HRMS, luminescence titration, and DFT calculations. The stabilization constant of the 1:1 complex formed Nd(III)-2OH-DAPhen in 0.4 M HNO₃ was determined to be 4.31 ± 0.04 . The FT-IR and ESI-HRMS spectra of the aqueous solution after complexation revealed that part of the nitrate anions participated in the inner coordination sphere of the complex. The luminescence titration method provided an interesting perspective for studying the structure of the complexes under strong acidic conditions. DFT calculations revealed that the 2OH-DAPhen ligand has a stronger affinity for Am(III), and Am–L complexes have more covalent interactions in bonding than Eu–L complexes. The proposed hydrophilic DAPhen ligands with simple structures could be synthesized by a facile process and have the outstanding affinity for An(III) over Ln(III), which provided a promising approach for the industrial separation of An(III)/Ln(III).

ASSOCIATED CONTENT

SI Supporting Information

The Supporting Information is available free of charge at <https://pubs.acs.org/doi/10.1021/acs.inorgchem.3c03331>.

Experimental details and supporting figures and tables ([PDF](#))

AUTHOR INFORMATION

Corresponding Authors

Ze-Yi Yan — Radiochemistry Laboratory, School of Nuclear Science and Technology, Lanzhou University, Lanzhou 730000 Gansu, China; orcid.org/0000-0001-9368-420X; Email: yanzeyi@lzu.edu.cn

Zhipeng Wang — Institute of Nuclear and New Energy Technology, Tsinghua University, Beijing 100084, China; Email: wangzhipeng@mail.tsinghua.edu.cn

Wei-qun Shi — Laboratory of Nuclear Energy Chemistry, Institute of High Energy Physics, Chinese Academy of Sciences, Beijing 100084, China; orcid.org/0000-0001-9929-9732; Email: shiwq@ihep.ac.cn

Authors

Qiang Wu — Radiochemistry Laboratory, School of Nuclear Science and Technology, Lanzhou University, Lanzhou 730000 Gansu, China

Huaixin Hao — Institute of Nuclear and New Energy Technology, Tsinghua University, Beijing 100084, China

Yang Liu — Laboratory of Nuclear Energy Chemistry, Institute of High Energy Physics, Chinese Academy of Sciences, Beijing 100084, China

Lei-Tao Sha — Radiochemistry Laboratory, School of Nuclear Science and Technology, Lanzhou University, Lanzhou 730000 Gansu, China

Wei-Jia Wang — Radiochemistry Laboratory, School of Nuclear Science and Technology, Lanzhou University, Lanzhou 730000 Gansu, China

Complete contact information is available at:

<https://pubs.acs.org/10.1021/acs.inorgchem.3c03331>

Author Contributions

#Q.W., H.H., and Y.L. contributed equally to this work.

Notes

The authors declare no competing financial interest.

ACKNOWLEDGMENTS

This work was financially supported by the National Natural Science Foundation of China (22176078 and 22376116).

REFERENCES

- (1) Wang, Z.; Lu, J.-B.; Dong, X.; Yan, Q.; Feng, X.; Hu, H.-S.; Wang, S.; Chen, J.; Li, J.; Xu, C. Ultra-efficient americium/lanthanide separation through oxidation state control. *J. Am. Chem. Soc.* **2022**, *144* (14), 6383–6389.
- (2) Wu, Q.; Zhang, F.; Yan, J.-X.; Sha, L.-T.; Huang, Q.-G.; Fu, X.; Li, Y.; Yan, Z.-Y. Extraction and immediate solidification of uranium (VI) using malonamide functionalized ionic liquids from H_2SO_4 -leaching liquor by specific self-assembly process. *J. Mol. Liq.* **2023**, *383*, 122148.
- (3) Yang, X.; Wu, W.; Xie, Y.; Hao, M.; Liu, X.; Chen, Z.; Yang, H.; Waterhouse, G. I. N.; Ma, S.; Wang, X. Modulating anion nanotrap via halogenation for high-efficiency $^{99}\text{TcO}_4^-/\text{ReO}_4^-$ removal under wide-ranging pH conditions. *Environ. Sci. Technol.* **2023**, *57* (29), 10870–10881.

(4) Liu, R.; Chen, G.; Wang, Z.; Zhao, Q.; Wu, L.; Li, Q.; Tian, R.; Chen, X.; Li, X.; Chen, Z.; Zhu, L.; Chen, J.; Duan, T. Calcium-intercalated zirconium phosphate by granulation: A strategy for enhancing adsorption selectivity of strontium and cesium from liquid radioactive waste. *Inorg. Chem.* **2023**, *62* (14), 5799–5809.

(5) Wu, Q.; Zhang, F.; Huang, Q.-G.; Fu, X.; Li, Y.; Li, X.-X.; Niu, Y.-N.; Yan, Z.-Y. A novel one-step strategy for extraction and solidification of Th(IV) based on self-assembly driven by malonamide-based $[\text{DC}_{18}\text{DMA}]^+$ ionic liquids. *Chem. Eng. J.* **2022**, *430*, 132717.

(6) Zhang, F.; Wu, Q.; Yan, J.-X.; Huang, Q.-G.; Li, Y.; Fu, X.; Li, X.-X.; Yan, Z.-Y. An integrated strategy for the extraction and solidification of Th(IV) ions from aqueous HNO_3 solution based on self-assembly triggered by $[\text{DODMA}]^+[\text{DGA}]^-$ ionic liquids. *Sep. Purif. Technol.* **2022**, *282*, 120111.

(7) Li, Y.; Li, X.-X.; Wang, Z.-Y.; Zhang, F.; Wu, Q.; Sha, L.-T.; Wang, Y.; Yan, Z.-Y. Design and synthesis of a novel bifunctional polymer with malonamide and carboxyl group for highly selective separation of uranium (VI). *Sep. Purif. Technol.* **2022**, *302*, 122115.

(8) Lewis, F. W.; Harwood, L. M.; Hudson, M. J.; Drew, M. G. B.; Desreux, J. F.; Vidick, G.; Bouslimani, N.; Modolo, G.; Wilden, A.; Sypula, M.; Vu, T. H.; Simonin, J. P. Highly efficient separation of actinides from lanthanides by a phenanthroline-derived bis-triazine ligand. *J. Am. Chem. Soc.* **2011**, *133* (33), 13093.

(9) Galluccio, F.; Macerata, E.; Weßling, P.; Adam, C.; Mossini, E.; Panzeri, W.; Mariani, M.; Mele, A.; Geist, A.; Panak, P. J. Insights into the Complexation mechanism of a promising lipophilic PyTri ligand for actinide partitioning from spent nuclear fuel. *Inorg. Chem.* **2022**, *61* (46), 18400–18411.

(10) Song, L.; Wang, X.; Li, L.; Wang, Z.; He, L.; Li, Q.; Pan, Q.; Ding, S. A novel type of tetradentate dipyridyl-derived bis(pyrazole) ligands for highly efficient and selective extraction of Am^{3+} over Eu^{3+} from HNO_3 solution. *Solvent Extr. Ion Exch.* **2023**, *41*, 119–142.

(11) Xiao, C.; Hassanzadeh Fard, Z.; Sarma, D.; Song, T. B.; Xu, C.; Kanatzidis, M. G. Highly efficient separation of trivalent minor actinides by a layered metal sulfide (KInSn_2S_6) from acidic radioactive waste. *J. Am. Chem. Soc.* **2017**, *139* (46), 16494–16497.

(12) Gorden, A. E.; DeVore, M. A.; Maynard, B. A. Coordination chemistry with f-element complexes for an improved understanding of factors that contribute to extraction selectivity. *Inorg. Chem.* **2013**, *52* (7), 3445–58.

(13) He, L.; Wang, X.; Li, Q.; Xiao, X.; Li, F.; Luo, F.; Pan, Q.; Ding, S. Novel water-soluble aromatic bisdiglycolamide masking agents for the separation of trivalent americium over lanthanides by NTAamide-(n-Oct) extractant. *J. Environ. Chem. Eng.* **2023**, *11* (2), 109536.

(14) Liu, C.; Lan, J.; Yan, Q.; Wang, Z.; Xu, C.; Shi, W.; Xiao, C. Temperature-responsive alkaline aqueous biphasic system for radioactive wastewater treatment. *Chin. Chem. Lett.* **2022**, *33* (7), 3561–3564.

(15) Cai, Y.; Wang, M.; Yuan, L.; Feng, W. Complexation and separation of palladium with tridentate 2,6-bis-triazolyl-pyridine ligands: synthesis, solvent extraction, spectroscopy, crystallography, and DFT calculations. *Inorg. Chem.* **2023**, *62* (23), 9168–9177.

(16) Lewis, F. W.; Harwood, L. M.; Hudson, M. J.; Geist, A.; Kozhevnikov, V. N.; Distler, P.; John, J. Hydrophilic sulfonated bis-1,2,4-triazine ligands are highly effective reagents for separating actinides(III) from lanthanides(III) via selective formation of aqueous actinide complexes. *Chem. Sci.* **2015**, *6* (8), 4812–4821.

(17) Edwards, A. C.; Mocilac, P.; Geist, A.; Harwood, L. M.; Sharrad, C. A.; Burton, N. A.; Whitehead, R. C.; Denecke, M. A. Hydrophilic 2,9-bis-triazolyl-1,10-phenanthroline ligands enable selective Am(III) separation: a step further towards sustainable nuclear energy. *Chem. Commun.* **2017**, *53* (36), 5001–5004.

(18) Xu, L.; Pu, N.; Li, Y.; Wei, P.; Sun, T.; Xiao, C.; Chen, J.; Xu, C. Selective separation and complexation of trivalent actinide and lanthanide by a tetradentate soft-hard donor ligand: solvent extraction, spectroscopy, and DFT calculations. *Inorg. Chem.* **2019**, *58* (7), 4420–4430.

- (19) Lemport, P. S.; Eviunina, M. V.; Matveev, P. I.; Petrov, V. S.; Pozdeev, A. S.; Khult, E. K.; Nelyubina, Y. V.; Isakovskaya, K. L.; Roznyatovsky, V. A.; Gloriozov, I. P.; Tarasevich, B. N.; Aldoshin, A. S.; Petrov, V. G.; Kalmikov, S. N.; Ustynyuk, Y. A.; Nenajdenko, V. G. 2-Methylpyrrolidine derived 1,10-phenanthroline-2,9-diamides: promising extractants for Am(III)/Ln(III) separation. *Inorg. Chem. Front.* **2022**, *9* (17), 4402–4412.
- (20) Yang, X.; Xu, L.; Zhang, A.; Xiao, C. Organophosphorus extractants: A critical choice for actinides/lanthanides separation in nuclear fuel cycle. *Chem. Eur. J.* **2023**, *29* (33), e202300456.
- (21) Zhang, H.; Li, A.; Li, K.; Wang, Z.; Xu, X.; Wang, Y.; Sheridan, M. V.; Hu, H.-S.; Xu, C.; Alekseev, E. V.; Zhang, Z.; Yan, P.; Cao, K.; Chai, Z.; Albrecht-Schönzart, T. E.; Wang, S. Ultrafiltration separation of Am(VI)-polyoxometalate from lanthanides. *Nature* **2023**, *616* (7957), 482–487.
- (22) Wu, F.; Lv, H.; He, X.; Cheng, Z.; Jia, H.; Xie, S.; Liu, Y.; Ye, G.; He, H. Selective Am(III) stripping with water-soluble PyTri-Diol in nitric acid from HDEHP organic phase. *J. Radioanal. Nucl. Chem.* **2020**, *323* (1), 283–289.
- (23) Yuan, T.; Xiong, S.; Shen, X. Coordination of actinide single ions to deformed graphdiyne: strategy on essential separation processes in nuclear fuel cycle. *Angew. Chem., Int. Ed.* **2020**, *59* (40), 17719–17725.
- (24) Panak, P. J.; Geist, A. Complexation and extraction of trivalent actinides and lanthanides by triazinylpyridine N-Donor ligands. *Chem. Rev.* **2013**, *113* (2), 1199–1236.
- (25) Dong, X.; Yan, Q.; Wang, Z.; Feng, X.; Chen, J.; Xu, C. Group Separation of hexavalent actinides from lanthanides through selective extraction by sterically hindered 2-ethylhexyl phosphonic acid mono-2-ethylhexyl ester. *Ind. Eng. Chem. Res.* **2022**, *61* (46), 17175–17182.
- (26) Ansari, S. A.; Pathak, P.; Mohapatra, P. K.; Manchanda, V. K. Chemistry of diglycolamides: promising extractants for actinide partitioning. *Chem. Rev.* **2012**, *112* (3), 1751–72.
- (27) Wang, Z.; Pu, N.; Tian, Y.; Xu, C.; Wang, F.; Liu, Y.; Zhang, L.; Chen, J.; Ding, S. Highly selective separation of actinides from lanthanides by dithiophosphinic acids: An in-depth investigation on extraction, complexation, and DFT calculations. *Inorg. Chem.* **2019**, *58* (9), 5457–5467.
- (28) Whittaker, D. M.; Griffiths, T. L.; Helliwell, M.; Swinburne, A. N.; Natrajan, L. S.; Lewis, F. W.; Harwood, L. M.; Parry, S. A.; Sharrad, C. A. Lanthanide speciation in potential SANEX and GANEX actinide/lanthanide separations using tetra-N-donor extractants. *Inorg. Chem.* **2013**, *52* (7), 3429–3444.
- (29) Huang, P.-W. Theoretical unraveling of the separation of trivalent Am and Eu ions by phosphine oxide ligands with different central heterocyclic moieties. *Dalton Trans.* **2022**, *51* (18), 7118–7126.
- (30) Tian, D.; Liu, Y.; Kang, Y.; Zhao, Y.; Li, P.; Xu, C.; Wang, L. A simple yet efficient hydrophilic phenanthroline-based ligand for selective Am(III) separation under high acidity. *ACS Cent. Sci.* **2023**, *9* (8), 1642–1649.
- (31) Khayambashi, A.; Chen, L.; Dong, X.; Li, K.; Wang, Z.; He, L.; Annam, S.; Chen, L.; Wang, Y.; Sheridan, M. V.; Xu, C.; Wang, S. Efficient separation between trivalent americium and lanthanides enabled by a phenanthroline-based polymeric organic framework. *Chin. Chem. Lett.* **2022**, *33* (7), 3429–3434.
- (32) Yang, X.-F.; Liu, Y.; Tao, W.-Q.; Wang, S.; Ren, P.; Yang, S.-L.; Yuan, L.-Y.; Tang, H.-B.; Chai, Z.-F.; Shi, W.-Q. Lipophilic phenanthroline diamide ligands in 1-octanol for separation of Am(III) from Eu(III). *J. Environ. Chem. Eng.* **2022**, *10* (5), 108401.
- (33) Xu, L.; Yang, X.; Zhang, A.; Xu, C.; Xiao, C. Separation and complexation of f-block elements using hard-soft donors combined phenanthroline extractants. *Coord. Chem. Rev.* **2023**, *496*, 215404.
- (34) Chen, B.; Liu, J.; Lv, L.; Yang, L.; Luo, S.; Yang, Y.; Peng, S. Complexation of lanthanides with *N,N,N',N'*-tetramethylamide derivatives of bipyridinedicarboxylic acid and phenanthrolinedicarboxylic acid: thermodynamics and coordination modes. *Inorg. Chem.* **2019**, *58* (11), 7416–7425.
- (35) Cao, H.; Wei, P.; Pu, N.; Zhang, Y.; Yang, Y.; Wang, Z.; Sun, T.; Chen, J.; Xu, C. Probing the difference in the complexation of trivalent actinides and lanthanides with a tridentate N,O-hybrid ligand: spectroscopy, thermodynamics, and coordination modes. *Inorg. Chem.* **2022**, *61* (16), 6063–6072.
- (36) Wang, Y.; Hu, B.; Li, Q.; Wu, Y.; Shang, X.; Yang, P.; Cai, Y.; Yuan, L.; Feng, W. Novel phenanthroline-derived pyrrolidone ligands for efficient uranium separation: Liquid-liquid extraction, spectroscopy, and molecular simulations. *J. Mol. Liq.* **2022**, *364*, 119909.
- (37) Song, L.; Wang, X.; Wang, D.; Xiao, Q.; Xu, H.; Li, Q.; He, L.; Ding, S. 2-Carboxamido-6-(1H-pyrazol-3-yl)-pyridines as ligands for efficient separation of americium(III) from europium(III). *Sep. Purif. Technol.* **2021**, *276*, 119262.
- (38) Jansone-Popova, S.; Ivanov, A. S.; Bryantsev, V. S.; Sloop, F. V.; Custelcean, R.; Popovs, I.; Dekarske, M. M.; Moyer, B. A. Bis-lactam-1,10-phenanthroline (BLPhen), a new type of preorganized mixed N,O-Donor ligand that separates Am(III) over Eu(III) with exceptionally high efficiency. *Inorg. Chem.* **2017**, *56*, 5911.
- (39) Velisek-Carolan, J. Separation of actinides from spent nuclear fuel: A review. *J. Hazard. Mater.* **2016**, *318*, 266–281.
- (40) Leoncini, A.; Huskens, J.; Verboom, W. Ligands for f-element extraction used in the nuclear fuel cycle. *Chem. Soc. Rev.* **2017**, *46* (23), 7229–7273.
- (41) Wang, H.; Cui, T.; Sui, J.; Mocilac, P.; Wang, Y.; Guo, Z. Efficient UO_2^{2+} extraction by DAPhens with asymmetric terminal groups: The molecular design, spectral titration, liquid-liquid extraction and mechanism study. *Sep. Purif. Technol.* **2022**, *282*, 120046.
- (42) Xiao, C.-L.; Wang, C.-Z.; Yuan, L.-Y.; Li, B.; He, H.; Wang, S.; Zhao, Y.-L.; Chai, Z.-F.; Shi, W.-Q. Excellent selectivity for actinides with a tetradebate 2,9-diamide-1,10-phenanthroline ligand in highly acidic solution: A hard–soft donor combined strategy. *Inorg. Chem.* **2014**, *53* (3), 1712–1720.
- (43) Geist, A.; Adnet, J.-M.; Bourg, S.; Ekberg, C.; Galán, H.; Guibaud, P.; Miguiditchian, M.; Modolo, G.; Rhodes, C.; Taylor, R. An overview of solvent extraction processes developed in Europe for advanced nuclear fuel recycling, part 1 — heterogeneous recycling. *Sep. Sci. Technol.* **2021**, *56* (11), 1866–1881.
- (44) Mossini, E.; Macerata, E.; Wilden, A.; Kaufholz, P.; Modolo, G.; Iotti, N.; Casnati, A.; Geist, A.; Mariani, M. Optimization and single-stage centrifugal contactor experiments with the novel hydrophilic complexant PyTri-Diol for the i-SANEX process. *Solvent Extr. Ion Exch.* **2018**, *36* (4), 373–386.
- (45) Macerata, E.; Mossini, E.; Scaravaggi, S.; Mariani, M.; Mele, A.; Panzeri, W.; Boubals, N.; Berthon, L.; Charbonnel, M.-C.; Sansone, F.; Arduini, A.; Casnati, A. Hydrophilic clicked 2,6-bis-triazolyl-pyridines endowed with high actinide selectivity and radiochemical stability: toward a closed nuclear fuel cycle. *J. Am. Chem. Soc.* **2016**, *138* (23), 7232–7235.
- (46) Herdzik-Koniecko, I.; Wagner, C.; Trumm, M.; Müllrich, U.; Schimmelpfennig, B.; Narbutt, J.; Geist, A.; Panak, P. J. Do An(III) and Ln(III) ions form heteroleptic complexes with diglycolamide and hydrophilic BT(B)P ligands in solvent extraction systems? A spectroscopic and DFT study. *New J. Chem.* **2019**, *43* (16), 6314–6322.
- (47) Wagner, C.; Müllrich, U.; Geist, A.; Panak, P. J. Selective extraction of Am(III) from PUREX raffinate: the AmSel system. *Solvent Extr. Ion Exch.* **2016**, *34* (2), 103–113.
- (48) Kaufholz, P.; Modolo, G.; Wilden, A.; Sadowski, F.; Bosbach, D.; Wagner, C.; Geist, A.; Panak, P. J.; Lewis, F. W.; Harwood, L. M. Solvent extraction and fluorescence spectroscopic investigation of the selective Am(III) complexation with TS-BTPhen. *Solvent Extr. Ion Exch.* **2016**, *34* (2), 126–140.
- (49) Ren, P.; Huang, P.-W.; Yang, X.-F.; Zou, Y.; Tao, W.-Q.; Yang, S.-L.; Liu, Y.-H.; Wu, Q.-Y.; Yuan, L.-Y.; Chai, Z.-F.; Shi, W.-Q. Hydrophilic sulfonated 2,9-diamide-1,10-phenanthroline endowed with a highly effective ligand for separation of americium(III) from europium(III): extraction, spectroscopy, and density functional theory calculations. *Inorg. Chem.* **2021**, *60* (1), 357–365.

- (50) Matveev, P.; Mohapatra, P. K.; Kalmykov, S. N.; Petrov, V. Solvent extraction systems for mutual separation of Am(III) and Cm(III) from nitric acid solutions. *A review of recent state-of-the-art.* *Solvent Extr. Ion Exch.* 2021, 39 (7), 679–713.
- (51) Zsabka, P.; Wilden, A.; Van Hecke, K.; Modolo, G.; Verwerft, M.; Cardinaels, T. Beyond U/Pu separation: Separation of americium from the highly active PUREX raffinate. *J. Nucl. Mater.* 2023, 581, 154445.
- (52) Ren, P.; Yan, Z.-Y.; Li, Y.; Wu, Z.-M.; Wang, L.; Zhao, L.-B.; Gao, Y.-Q.; Wu, W.-S. Synthesis and characterization of bisdiglycolamides for comparable extraction of Th⁴⁺, UO₂²⁺ and Eu³⁺ from nitric acid solution. *J. Radioanal. Nucl. Chem.* 2017, 312 (3), 487–494.
- (53) Guo, Y.; Wang, R.-Y.; Kang, J.-X.; Ma, Y.-N.; Xu, C.-Q.; Li, J.; Chen, X. Efficient synthesis of primary and secondary amides via reacting esters with alkali metal amidoboranes. *Nat. Commun.* 2021, 12 (1), 5964.